

Received July 29, 2021, accepted August 11, 2021, date of publication August 24, 2021, date of current version September 10, 2021.

Digital Object Identifier 10.1109/ACCESS.2021.3107575

The Expected Values of Self- and Mutual Impedances of Overhead Lines and Impacts of on Sags and Phase Conductor Imbalances: Part 2

INSU KIM , (Member, IEEE)

Department of Electrical Engineering, Inha University, Incheon 22212, South Korea

e-mail: insu@inha.ac.kr

This work was supported in part by the National Research Foundation of Korea Basic Science Research Program under Grant NRF-2019R1F1A1061259, and in part by the Korean Ministry of Oceans and Fisheries under Project 1525011610 and Project KIMST-20210629.

ABSTRACT This paper presents a method that finds the expected values of self- and mutual impedances of overhead lines with the uncertainties such as the ground resistivity, conductor characteristics, and transmission line structures. For this purpose, this study designs a stochastic random sampling method that removes the uncertainties. A finite element analysis method that includes a single logarithmic closed-form solution to Carson's improper integral is adopted. The impact of an increase in sags and an imbalance in phase conductors on self- and mutual impedances is examined. As a result, the expected values of the self- and mutual impedances of an overhead line are evaluated. It is also shown that as the sag ratio increases, the self- and mutual impedances decrease.

INDEX TERMS Carson's integral, closed-form solution, self- and mutual impedances, finite element method, Monte Carlo simulation.


NOMENCLATURE

ABBREVIATIONS

CDER = complex depth of earth return.
EM = electromagnetic.
EV = expected value.
FEM = finite element method.
GMR = geometric mean radius.
GMD = geometric mean distance.
LB = lower bound.
OL = overhead line.
SLA = single logarithm approximation.
TEM = transverse electromagnetic.
UB = upper bound.

VARIABLES

C_{method} and D_{method} = cost function and relative difference of a specific impedance calculation method.
 σ_g = conductivity of the ground.
 ϵ_0 , ϵ_g , and ϵ_r = dielectric permittivity of vacuum, permittivity of the ground, and relative permittivity of the ground.

The associate editor coordinating the review of this manuscript and approving it for publication was Arpan Kumar Pradhan .

μ_0 , μ_g , and μ_r = permeability of vacuum, permeability of the ground, and relative permeability of the ground.
 H = horizontal tension in the conductor at the maximum deflection point.
 l = conductor length or span.
 λ = integration variable.
 N_{row} and N_{col} = total number of rows and columns of impedance matrix.
 r_i = radius of conductor i .
 ρ = ground resistivity in $\Omega\cdot\text{m}$.
 s = sag length of the conductor.
 θ_{ij} = expected value of the i th row and j th column in the impedance matrix.
 w = weight per unit length of the conductor.
 z_{eq} = total equivalent impedance.
 z_k = impedance in the k th element in the finite element method.
 \hat{z}_k = impedance in the k th variable-sized element.
 $\hat{z}_{s,k}$ and $\hat{z}_{m,k}$ = self- and mutual impedances in the k th variable-sized element.

- \mathbf{Z}_{ij} = the i th row and j th column in the 3 by 3 impedance matrix.
- \mathbf{Z}_{ref} = 3 by 3 impedance matrix defined as the reference case.
- $\mathbf{Z}_{\text{method}}$ = 3 by 3 impedance matrix determined by a specific impedance calculation method.

I. INTRODUCTION

Carson derived the propagation equations of electromagnetic waves along sufficiently long overhead lines (OLs) [1]. The equations including the improper integral can calculate the self- and mutual impedance of OLs. The integral, in the form of the Struve function and the second kind Bessel function [2], was solved by infinite series and asymptotic expansions [1]. Thus, many studies have approximated a closed-form solution. For example, a single-logarithmic closed-form solution was presented in [3]–[6], which is referred to as the complex depth of earth return (CDER) model. The accuracy of the CDER method was improved in [7], [8], which is referred to as a single logarithmic approximation (SLA) model. A double logarithmic approximation was also presented in [9], which was improved in [10]. Recently, the accuracy of the various closed-form solutions was compared in [11]. In that sense, closed-form solutions have been widely used because of their easy applicability.

The integral presented by Carson was also solved by numerical integration in [12], [13]. For example, the accuracy of such a numerical integration method was verified by the finite element method (FEM) in [14]. However, these methods ignored the sags of OLs. For example, a method that calculates the sag and tension of OLs as the classical graphic method was presented in [15]. The effect of the sag of OLs suspended by towers with identical heights and spans on electromagnetic (EM) field was examined in [16], [17]. The EM field for more realistic OLs with unequal height towers and unequal spans was also calculated in [18], [19]. In most studies, the FEM has been commonly applied for EM field estimating problems, but none of the above studies examined the effect of the sag on the self- and mutual impedance of OLs by using the SLA improved in [8]. Thus, this study modifies a FEM so that it can examine the effect of the sags and phase conductor imbalances of OLs on self- and mutual impedances. For this purpose, this study designs a two-step variable-sized FEM that calculates the self- and mutual impedances of parallel conductors. This study also integrates the compensated SLA method validated in [8] into the proposed FEM, so it can examine the more accurate effect of sages on impedance. The proposed method can be not only applied to multi-phase OLs with equilateral and inequilateral conductor dispositions but also valid for an OL with a weak sag.

The self- and mutual impedances of OLs at different resistances, permeabilities, and permittivities of the conductor, air, and ground were calculated in [20]. Uncertainties in elasticity modulus and conductor creep values showed a weak effect on

actual sag values of OLs. In contrast, conductor temperature and sag values showed a significant effect on sag calculation errors [21]. Uncertainties in the dynamic thermal rating of OLs were examined by a combination of affine arithmetic and probabilistic optimal power flow models [22]. The previous studies did not take the uncertainty in conductor heights into account. Thus, the uncertainty in heights of OLs was removed by examining the effect of the height on EM calculation results by the image charge method in two dimensions [23]. However, none of the above studies examined the effect of the uncertainties in frequency, ground resistivity, conductor characteristics, and transmission line structures on self- and mutual impedances of OLs with equilateral and inequilateral conductor dispositions. Thus, the second objective of this study is to estimate the expected value (EV) of the self- and mutual impedances of OLs with the uncertainties such as frequency, ground resistivity, conductor characteristics, and transmission line structures. For this, this study presents a stochastic random number-based simulation model, or Monte Carlo simulation. Then, the proposed stochastic method finds (a) the EVs of self- and mutual impedances of OLs with the uncertainties, (b) a maximum accuracy improvement case of the SLA presented in [8], and (c) correlation coefficients of the uncertainties on the self- and mutual impedances.

The rest of the paper is organized as follows: Section 2 presents the problem statement. In section 3, an overview of the SLA closed-form solutions is presented. Sections 4 and 5 provide the proposed FEM and stochastic simulation models. In Section 6, the numerical results are evaluated. Finally, section 7 summarizes the major findings of this paper.

II. PROBLEM STATEMENT

In the quasi-TEM (transverse electromagnetic) mode of propagation, Carson defined the ground return impedance of OLs in terms of an improper integral. Carson's solution, necessary to be expanded into infinite series, and many other closed-form approximations can be used to estimate an EV of the self- and mutual impedances of OLs. The EVs are defined by

$$\theta_{ij} = E[\mathbf{Z}_{ij}], \quad (1)$$

where

θ_{ij} = EV of the i th row and j th column (e.g., ii corresponds to the self-impedance and ij the mutual impedance of an OL).

To calculate the EV of the self- and mutual impedances for OLs, the uncertainties in the frequency, ground resistivity, conductor characteristics (e.g., geometric mean radius [GMR] and dc resistance), and transmission line structures (e.g., a single, double, or more circuit structure, and geometric mean distance [GMD]) should be taken into account. Other uncertainties also include a line sag and an imbalance in phase conductors. To remove the uncertainties, this study presents a stochastic random sampling method, or Monte Carlo simulation, which is combined by a two-step variable-sized FEM. In the proposed method, the self- and mutual impedances are calculated by the

following closed-form approximation methods proposed in the literature.

III. CARSON'S GROUND RETURN IMPEDANCE

The two conductors in parallel in each other are presented in Fig. 1. In the air with ϵ_0 and μ_0 , the EM properties of the ground are defined by $\epsilon_g = \epsilon_r \epsilon_0$, $\mu_g = \mu_r \mu_0$, and σ_g . The propagation constant of the ground is given as:

$$\gamma_g = \sqrt{j\omega\mu_g(\sigma_g + j\omega\epsilon_g)}. \tag{2}$$

For a TEM mode of propagation, Carson defined the formula of the mutual impedance [1]:

$$Z_m = \frac{j\omega\mu_0}{2\pi} \left(\ln \left(\frac{D_{ij}}{d_{ij}} \right) + J_m \right), \tag{3}$$

$$J_m = \int_0^\infty \left(\frac{2e^{-H\lambda}}{\lambda + \sqrt{\lambda^2 + \gamma_g^2}} \right) \cos(x_{ij}\lambda) d\lambda, \tag{4}$$

where

$$D_{ij} = \sqrt{(h_i + h_j)^2 + x_{ij}^2}, d_{ij} = \sqrt{(h_i - h_j)^2 + x_{ij}^2}, \text{ and } H = h_i + h_j.$$

The self-impedance can be also derived from (4) by setting $d_{ij} = r_i$ (the radius of the conductor i), $D_{ij} = 2h_i$, $H = 2h_i$, and $x_{ij} = 0$.

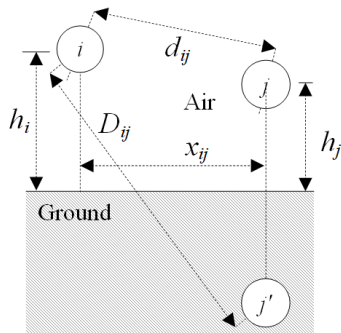


FIGURE 1. Two-conductor example located in parallel in the air.

Carson presented the solution of the improper integral of (4) in the form of the Struve function and the second kind Bessel function [1], [24]. Since Carson's solution includes the infinite series, many studies have presented closed-form approximation solutions.

A. DUBANTON'S CLOSED-FORM

The SLA simplifies the improper integral of (4) [3]–[6],

$$Z_s \approx \frac{j\omega\mu_0}{2\pi} \ln \frac{(2h_i + 2p)}{r_i}, \tag{5}$$

$$Z_m \approx \frac{j\omega\mu_0}{2\pi} \ln \frac{\sqrt{(H + 2p)^2 + x_{ij}^2}}{d_{ij}}, \tag{6}$$

$$p = \gamma_g^{-1}. \tag{7}$$

This method, added by $2p$, is also referred to as the CDER method.

B. ALVARADO–BETANCOURT'S CLOSED-FORM

The accuracy of the CDER method, or (5) and (6), was improved in [7],

$$J_m \approx \frac{1}{2} \ln \left(\frac{\left(1 + \frac{p}{H/2}\right)^2 + \beta^2}{1 + \beta^2} \right) - \frac{1}{24} \left(\frac{1}{\left(\frac{H}{2p}(1 + j\beta) + 1\right)^3} + \frac{1}{\left(\frac{H}{2p}(1 - j\beta) + 1\right)^3} \right), \tag{8}$$

where

$$H = h_i + h_j \text{ and } \beta = x_{ij}/H.$$

The self-impedance is also derived by setting $x_{ij} = 0$ and $h_i = h_j$.

C. COMPENSATED SINGLE LOGARITHMIC APPROXIMATION

A compensated SLA was presented in [8],

$$J_s \approx -\frac{1}{2} \ln(q_1) + \frac{1}{2} \ln(q_1 + 1) - \frac{1}{24}(q_1 + 1)^{-3} + \frac{12}{5}(2q_1 + 5)^{-5}, \tag{9}$$

$$J_m \approx -\frac{1}{2} \ln(q_2) + \frac{1}{4} \ln\left(q_2 + \frac{1}{1 + j\beta}\right) + \frac{1}{4} \ln\left(q_2 - \frac{1}{-1 + j\beta}\right) + J_1 + J_2, \tag{10}$$

where

$$q_1 = \frac{h_i}{p}, \tag{11}$$

$$q_2 = (h_i + h_j)/2p. \tag{12}$$

The detailed derivations of J_1 and J_2 terms are presented in [8].

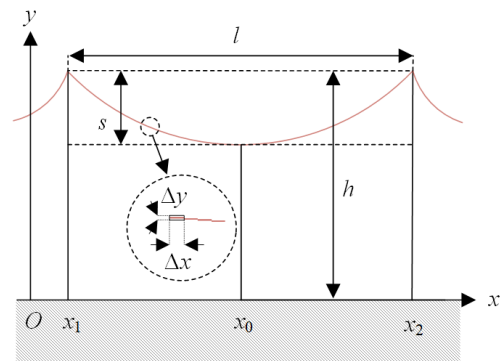


FIGURE 2. Line sag and span.

IV. PROPOSED LINE SAG MODELING

A. LINE SAG AND SPAN

Sag and tension in OLs depend on the span of the conductor. For example, the sag of the conductor, s , suspended by the

two same height poles in Fig. 2 is proportional to the weight per unit length, w , and the square of the distance between the two poles, l , and inversely proportional to the horizontal tension (H) at the maximum deflection point (at x_0) [15]. That is, the shape of the conductor can be approximated by the following parabola expressed on the x - y plane:

$$y(x) \approx \frac{wl^2}{8H} = \frac{w(x-x_0)^2}{8H} \quad \text{for } x_1 \leq x \leq x_2. \quad (13)$$

B. PROBLEM FORMULATION

An OL consisting of three parallel conductors for phases a , b , and c of carrying each phase current is considered in Fig. 2. The self- and mutual impedances of the three parallel conductors are calculated by the two-step variable-sized FEM, the detailed procedures of which are presented in the next section. The OL is divided by N elements in the x - y plane. In such a case, the following procedures calculate the self- and mutual impedances of the OL:

- An element of three parallel conductors for phases a , b , and c carries the arbitrary-amplitude sinusoid currents, but the other elements are set to carry zero currents.
- To approximate the line sag shape described in (12), Δx and Δy are sufficiently small.
- Using the two-step variable-sized FEM, the k th self- and mutual impedances are calculated. This step is repeated until calculating the N th element. If a double or more circuit model is considered, the number of phase conductors of an OL increases. Therefore, the proposed problem is reduced into that of calculating the self- and mutual impedances of the OL in per unit length, which can be solved by the following proposed FEM.

C. TWO-STEP VARIABLE-SIZED FINITE ELEMENT METHOD

The FEM has been applied for unbounded EM potential problems in several approaches. The approaches include the discretization method [25], Green's integral formula [26], or multigrid methods. For the same reasons as the EM field estimation problem of an OL [14], the first method is adopted in this paper.

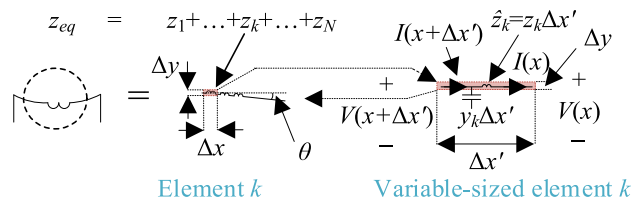


FIGURE 3. Proposed two-step FEM.

In the previous OL consisting of the three parallel conductors for phases a , b , and c and N elements in Fig. 2, let the total equivalent impedance of the OL with span l be z_{eq} . The impedance (z_{eq}) can be the summation of each small line impedance, z_k ($k = 1, 2, \dots, N$), for the OL with a slight sag with the angle of θ in Fig. 3. Additionally, let the self- or

mutual impedance be \hat{z}_k for the k th element of the OL with a sag. If each \hat{z}_k is known ($k = 1, 2, \dots, N$), z_{eq} can be approximated by

$$z_{eq} = \sum_{k=1}^N z_k \approx \sum_{k=1}^N \frac{\hat{z}_k}{(\Delta x' / \Delta x)}. \quad (14)$$

To determine each \hat{z}_k , the discretization method in [25] is modified in the following steps and assumptions:

- The discretization area includes a square of $\Delta x \times \Delta y$, used in the first step, and $\Delta x' \times \Delta y$, used in the second step. In the second step, the OL in the k th element is assumed to be sufficiently long enough to neglect the end effects. In other words, $\Delta x'$ in Fig. 2 is sufficiently long.
- The proposed method iteratively calculates the self- and mutual impedances ($\hat{z}_{s,k}$ and $\hat{z}_{m,k}$) of \hat{z}_k . For example, \hat{z}_k can be approximated by

$$\hat{z}_{s,k} \approx \frac{j\omega\mu_0}{2\pi} \left(\ln \left(\frac{2h_{i,k} + 2p}{r_i} \right) \right) \quad (k = 1, 2, \dots, N), \quad (15)$$

$$\hat{z}_{m,k} \approx \frac{j\omega\mu_0}{2\pi} \left(\ln \left(\frac{\sqrt{(h_{i,k} + h_{j,k} + 2p)^2 + x_{ij,k}^2}}{\sqrt{(h_{i,k} - h_{j,k})^2 + x_{ij,k}^2}} \right) \right) \quad (k = 1, 2, \dots, N). \quad (16)$$

- Then, $\hat{z}_{s,k}$ and $\hat{z}_{m,k}$ are scaled down by the ratio of Δx and $\Delta x'$ in (13).

The continuity requirement between neighboring finite elements is solved by setting Δx and Δy to be sufficiently small. Writing a KVL equation for the element in Fig. 3 gives

$$V(x + \Delta x') = V(x) + z_k \Delta x' I(x). \quad (17)$$

The solutions of (14) and (15) satisfy the condition of (16). For simplicity, bundled conductors are neglected. However, the proposed method can be extended to the bundled conductors. The conductors are assumed to be the uniform equal size in every element. The proposed method is valid for an OL with a weak sag, in other words, if a sag ratio of s to h in Fig. 2 is small.

V. PROPOSED UNCERTAINTY DESIGN

A. STOCHASTIC METHOD FOR FINDING EV

This study is to find the EV of self- and mutual impedances of OLs. To determine the EV, the following uncertainties should be considered as a random variable: Frequency, ground resistivity, conductor characteristics (e.g., GMR and dc resistance), and transmission line structures (e.g., a single, double, or more circuit structure, and GMD). To remove the uncertainties in the random variables, a stochastic Monte Carlo simulation is proposed in the following steps:

Step 1 Initialization: The representative intervals of the frequency, ground resistivity, conductor characteristics, and transmission line structures are defined as an upper bound (UB) and lower bound (LB) for practical OLs.

Step 2 Random Selection of an Overhead Line The total number of samples of OLs is selected as sufficiently large at the logarithmic scale. For example, the total number of samples is 10^6 , which is selected by trial and error because simulation beyond 10^6 samples takes long time to complete at a laptop computer (e.g., HP ZBook, Intel i7-7700HQ CPU @ 2.80GHz, 16.0 GB memory, and MATLAB 2019b). This study generates uniformly distributed random numbers for the polyhedral uncertainty set (e.g., the ground resistivity, overhead line structure, and cable) within UBs and LBs. Then, each case randomly selects the OL structure (e.g., a single or double line circuit), the position of phase conductors (e.g., GMD), the cable characteristics (e.g., GMR and dc resistance), the ground resistivity, and the frequency.

Step 3 Calculation of Self- and Mutual Impedances: The self- and mutual impedances of each OL are calculated using one of the previous methods.

Step 4 Termination: The previous steps 2 and 3 are repeated until to complete the total number of OLs.

B. MATHEMATICAL FORMULATION OF FINDING EV

The relative difference (D_{method}) to the reference impedance is defined by

$$D_{method,ij}(\%) = \frac{||\mathbf{Z}_{ref,i,j} - \mathbf{Z}_{method,i,j}||}{|\mathbf{Z}_{ref,i,j}|}, \quad (18)$$

where

\mathbf{Z}_{ref} = 3 by 3 impedance matrix as the reference

\mathbf{Z}_{method} = 3 by 3 impedance matrix determined by one of the previous methods.

The cost function (C_{method}) is also defined by the average of the relative difference,

$$C_{method} = \frac{\sum_{i=1}^{N_{row}} \sum_{j=1}^{N_{col}} D_{method,ij}}{N_{row}N_{col}}, \quad (19)$$

where N_{row} and N_{col} = total number of rows and columns of impedance matrix \mathbf{Z} (e.g., 3).

The objective of the proposed stochastic method is to calculate the accurate EV by minimizing the cost function (e.g., in (18)),

$$Minimize C_{method,i}, \quad (20)$$

TABLE 1. Stochastic Simulation Design for an EV Estimation Problem of Self- and Mutual Impedances of an Overhead Line.

Random variable	Interval
Frequency	60 Hz (fixed for power system applications)
Ground resistivity (ρ)	1 Ω -m to 10 k Ω -m [10]
Cable specification	ACSR cable from Joree to Partridge in [30]
Structure [23, 31, 32]	Single and double circuits
Method	Monte Carlo simulation
Maximum sample size	10^6 (Selected by trial and error)
Length	100 km
Base MVA	100 MVA
Base voltage	138 kV (line-to-line)

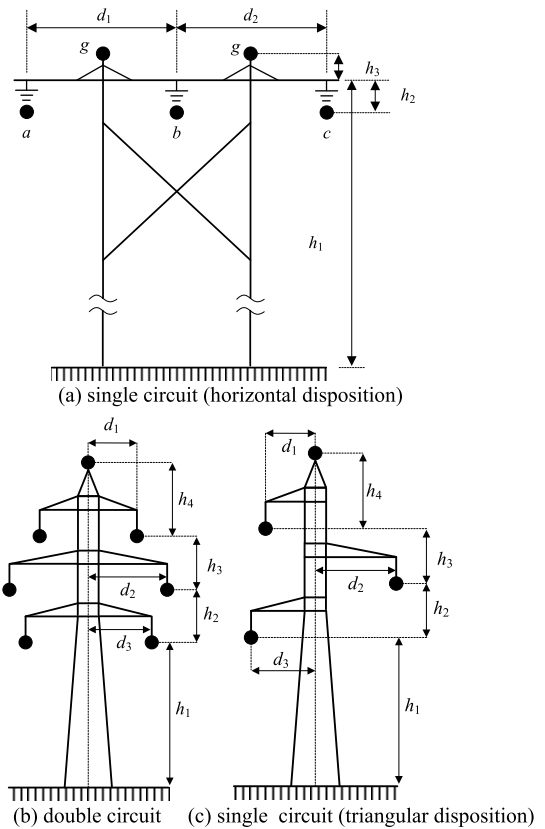


FIGURE 4. Tower structures.

where $C_{method,i}$ = cost function at the i th Monte Carlo simulation case, $i = 1, \dots, N$, and N = number of the total cases.

In other words, if the proposed stochastic method finds the impedance close to the reference impedance (\mathbf{Z}_{ref}), the cost function is minimized. The variance in the cost functions is also minimized,

$$Minimize Var[C_{method,i}]. \quad (21)$$

VI. NUMERICAL RESULTS

A. EXPECTED VALUE OF SELF- AND MUTUAL IMPEDANCES

The reference impedance (\mathbf{Z}_{ref}) is defined by calculating up to the 24th high-order terms of the infinite series presented in [8], [27], [28]. In [8], the impedance determined by the compensated SLA was closest to the reference impedance through the two-conductor, distribution line, and transmission line examples [8]. Thus, this study integrates the compensated SLA method into the proposed FEM.

In the EV estimation problem, the stochastic method (i.e., Monte Carlo simulation) for the ground resistivity, overhead line structure, and cable is proposed with polyhedral uncertainty sets, which enable the most straightforward “tractable” representation [29]. For example, an OL consists of a single or double circuit with ACSR cables. The representative interval of ACSR cable specifications such as GMR and dc resistance is presented in the Appendix in [30]. Types of towers and

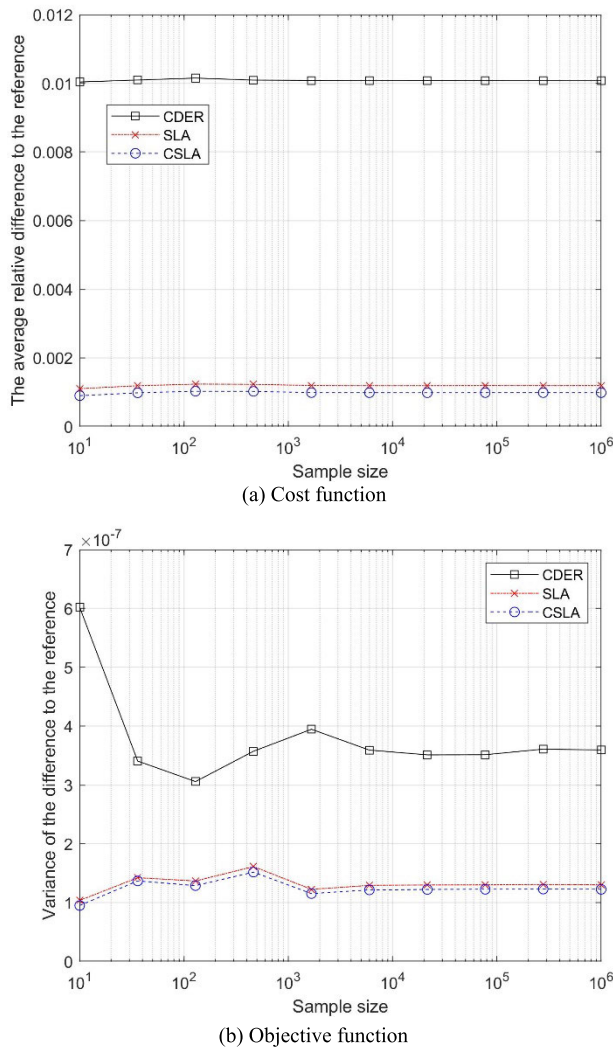


FIGURE 5. Cost and objective functions (equilateral conductor disposition).

positions of cables are presented in Fig. 4, which can be classified as the equilateral (e.g., Fig. 4 (a) and (b)) and inequilateral type (e.g., Fig. 4 (c)). The intervals of the single and double circuit structures such as an UB and LB of vertical and horizontal distances of phase conductors are presented in [23], [31], [32]. The detailed simulation parameters are presented in TABLE 1.

In EV estimation Monte Carlo simulations, the total number of OLS increases at the logarithmic scale (e.g., 10 to 10^6). Each case randomly estimates the self- and mutual impedances of the OL with the polyhedral uncertainty sets described in TABLE 1. That is, this study generates uniformly distributed random numbers in the polyhedral uncertainty set. For example, an OL initially picks its structure type (e.g., a single or double circuit in Fig. 4) and then picks its random distances of phase conductors (e.g., the horizontal and vertical distances) and cable specifications (e.g., GMR and dc resistance). In the EV estimation problem, the OL with a length of 100 km at a line-to-line voltage of 138 kV, a base of 100 MVA, and a frequency of 60 Hz is assumed.

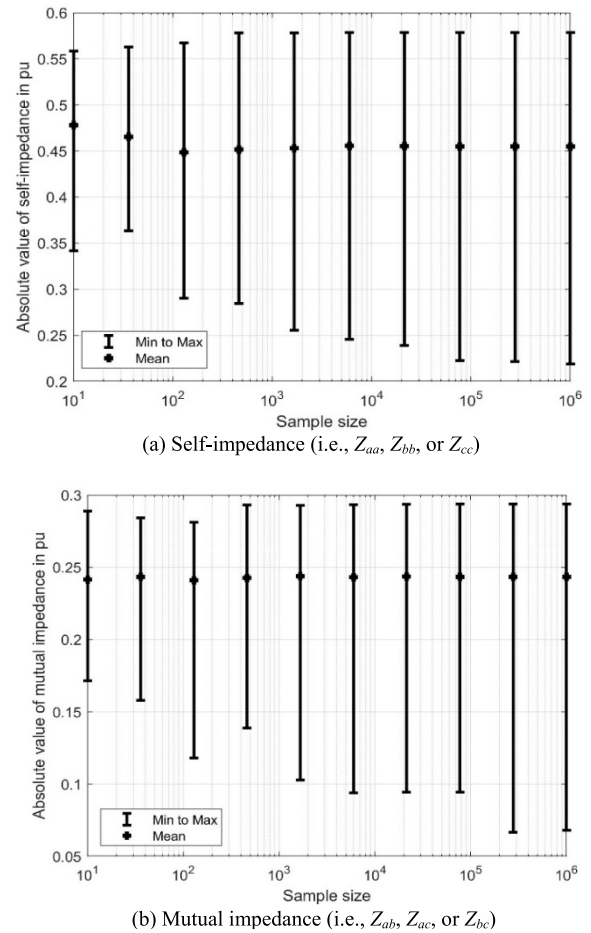


FIGURE 6. EV of self- and mutual impedances of an overhead line with equilateral conductor disposition.

B. EQUILATERAL CONDUCTOR DISPOSITION

In the EV estimation of impedance of OLS with the equilateral conductor disposition (e.g., Fig. 4 (a) and (b)), the cost function is the average of the relative differences to the 3 by 3 reference impedance matrix (\mathbf{Z}_{ref}) in Fig. 5 (a). The compensated SLA method (denoted as CSLA by the circle symbol) shows the least cost at the sample size from 10 to 10^6 . The detailed equations of the compensated SLA method are presented in [8]. In other words, the compensated SLA method successfully improves the previous SLA method, so its average relative difference to the reference is located lower than that of the previous SLA method (denoted as SLA by in the cross symbol).

The second objective function is to minimize the variance in the average of the relative differences to the reference impedance, defined in (20). Fig. 5 (b) compares the variance in the relative differences as the sample size increases from 10 to 10^6 . The compensated SLA method shows the least cost function, or in Fig. 5 (a), and the least objective function, or in Fig. 5 (b), when compared to the previous CDER and SLA methods.

In Fig. 6 (a), as the sample size increases, the EV of the self-impedance of the OL with a length of 100 km converges

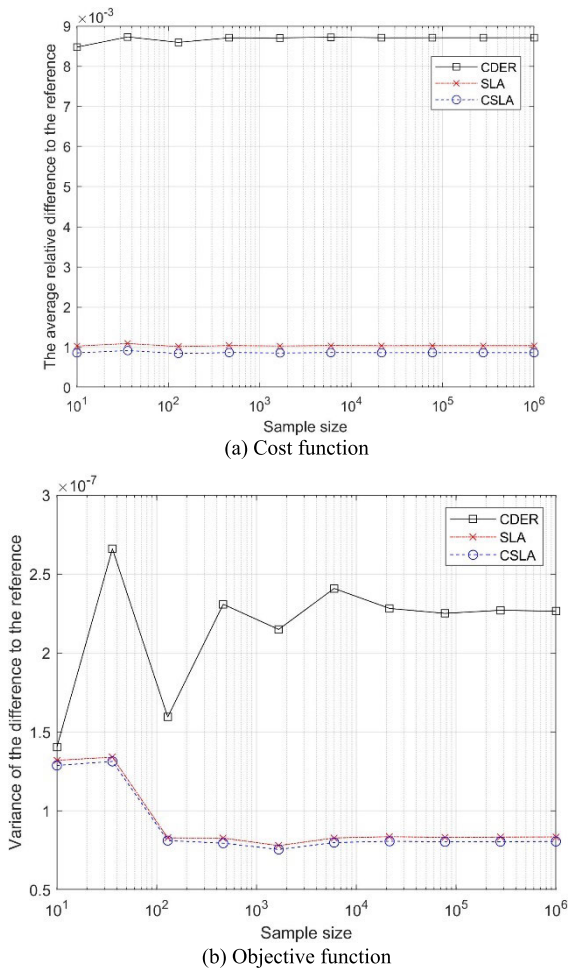


FIGURE 7. Cost and objective functions (inequilateral conductor disposition).

to $0.0668 + j0.4501$ p.u., at the LB of $0.0166 + 0.2182j$ p.u. and the UB of $0.1563 + 0.5572j$ p.u. The EV of the mutual impedance in Fig. 6 (b) converges to $0.0304 + 0.2416j$ p.u., at the LB of $0.0182 + 0.0655j$ p.u. and the UB of $0.0306 + 0.2922j$ p.u.

C. INEQUILATERAL CONDUCTOR DISPOSITION

This study evaluates EVs of self- and mutual impedances of OLs with the inequilateral conductor disposition (e.g., the triangular shape in Fig. 4 (c)). The intervals of the circuit structure such as an UB and LB of vertical and horizontal distances of phase conductors are presented in [23]. In Fig. 7 (a), the average relative difference to the reference of the compensated SLA method (denoted as CSLA by the circle symbol) is the lowest when the sample size varies from 10 to 10^6 , which means that the compensated SLA method improves the previous SLA method, denoted as SLA in the cross symbol. In Fig. 7 (b), the variance in the average of the relative differences to the reference impedance is minimized when the compensated SLA method is used. Thus, the inequilateral conductor disposition case shows the same results as the equilateral conductor disposition case.

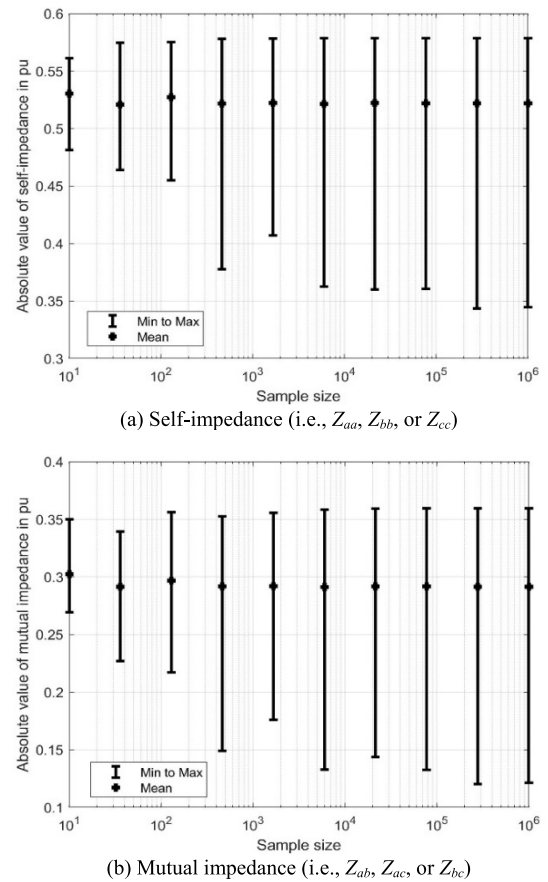


FIGURE 8. EV of self- and mutual impedances of an overhead line with inequilateral conductor disposition.

TABLE 2. Maximum Relative Difference Improvement.

Method	Impedance (Z_{ac}) in $\Omega/100$ km	Relative difference (%)
Z_{ref}	$4.869+17.907i$	-
Z_{CDER}	$5.013+18.224i$	1.8548 %
Z_{SLA}	$4.852+17.838i$	0.3843 %
Z_{CSLA}	$4.854+17.846i$	0.3366 %

As the main objective of this paper, this study evaluates EVs of self- and mutual impedances of OLs with the inequilateral conductor disposition. In Fig. 8 (a), the EV of the self-impedance of the OL with a length of 100 km converges to $0.0792 + j0.5160$ p.u., at the LB of $0.0250 + 0.3439j$ p.u. and the UB of $0.1565 + 0.5570j$ p.u. The EV of the mutual impedance in Fig. 8 (b) converges to $0.0308 + 0.2899j$ p.u., at the LB of $0.0217 + 0.1195j$ p.u. and the UB of $0.0309 + 0.3583j$ p.u.

D. EFFECT OF THE COMPENSATED SLA ON RELATIVE DIFFERENCE

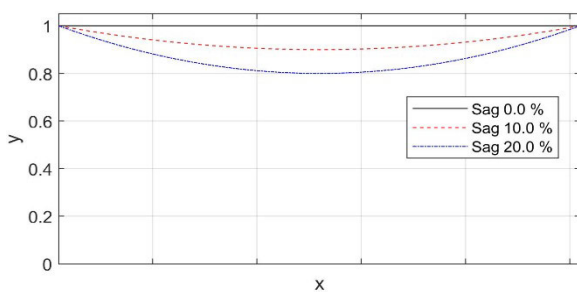
Many studies introduced in the related literature survey have verified their accuracy in calculating self- and mutual impedances. However, they ignored the uncertainties in the position of the phase conductors and the cable characteristics. The compensated SLA method proposed in [8] improved slightly the accuracy of the previous models. For example,

TABLE 3. Correlation Coefficients of Random Variables for Absolute Value of Impedance.

Conductor disposition	Method	Ground Resistivity (ρ)	d_{ij}	GMR	DC resistance
Equilateral	Reference	0.5087	-0.1134	-0.0802	0.0825
	CDER	0.5091	-0.1125	-0.0800	0.0824
	SLA	0.5087	-0.1131	-0.0801	0.0825
	CSLA	0.5087	-0.1131	-0.0801	0.0825
Inequilateral	Reference	0.7070	-0.1831	0.1039	0.1031
	CDER	0.7073	-0.1827	0.1036	0.1029
	SLA	0.7068	-0.1832	0.1038	0.1031
	CSLA	0.7069	-0.1832	0.1038	0.1031

the compensated SLA model (denoted as $\mathbf{Z}_{\text{proposed}}$ in [8]) decreased an average of the relative difference of the previous SLA model (\mathbf{Z}_{SLA}) from 0.02952 to 0.02684% in the second case study in [8].

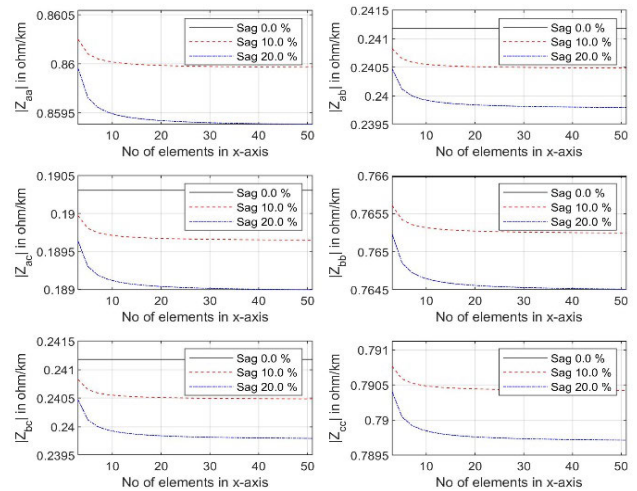
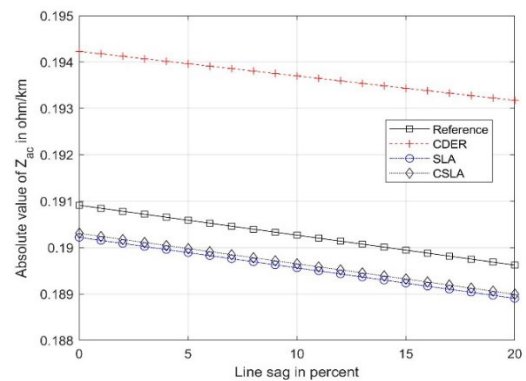
To analyze the effect of the compensated SLA (e.g., \mathbf{Z}_{SLA}) in [8] on the accuracy improvement to the previous models (e.g., \mathbf{Z}_{CDER} and \mathbf{Z}_{SLA}), this study searches the maximum accuracy improvement through all the Monte Carlo simulation runs. TABLE 2 presents the maximum relative difference improvement. At the frequency of 60 Hz, the maximum improvement of the compensated SLA in the relative difference to the reference impedance (\mathbf{Z}_{ref}) is 0.3366 percent for the impedance Z_{ac} of the OL consisting of Cardinal cables with a GMD of 17.281 m, a GMR of 0.012 m, and a dc resistance of 0.067 Ω/km , on the ground with a resistivity of 8.6 $\Omega\cdot\text{m}$. For example, when compared to a relative difference of 0.3843 percent of the SLA method and a relative difference of 1.8548 percent of the CDER method, the more accurate impedance (e.g., a relative difference of 0.3366 percent) can be used as input for other research purposes such as transient simulations.

**FIGURE 9. Sag in an overhead line.**

E. CORRELATION COEFFICIENTS OF UNCERTAINTY RANDOM VARIABLES

To analyze the correlation effect of the uncertainty random variables on the self- and mutual impedances, correlation coefficients of each uncertainty (ground resistivity, d_{ij} , GMR, and dc resistance, excluding the frequency) to the absolute value of the impedance are presented in TABLE 3.

For both the equilateral and inequilateral conductor dispositions, the ground resistivity indicates a positive correlation for the self- and mutual impedances because of the $2p$ term

**FIGURE 10. Self- and mutual impedance convergence when the number of elements in the x-axis increases.****FIGURE 11. Absolute value of Z_{ac} when the sag ratio increases.**

in (5) and (6), which is proportional to the square root of the ground resistivity. The d_{ij} term shows a weak negative correlation. In fact, the mutual impedance is logarithmically inversely proportional to the d_{ij} term in (21). GMR and dc resistance do not show a correlation to the impedance.

F. IMPACT OF LINE SAGS AND PHASE IMBALANCE

To take an increase in line sags and an imbalance in phase conductors into account, this study performs Monte Carlo simulations up to 10^5 total cases. In this simulation, this study adds the uncertainty that each phase conductor can select a different cable in TABLE 1, which models an imbalance in phase conductors. At the frequency of 60 Hz, the maximum improvement of the compensated SLA in the relative difference to the reference impedance is 0.3167 percent for the impedance Z_{ac} of the OL consisting of Partridge, Finch, and Flamingo cables with a GMD of 17.052 m, at a ground resistivity of 9.5 $\Omega\cdot\text{m}$. Then, the self and mutual impedances of the OL with a length of 1 km are calculated at the sag ratios of 0, 10, and 20 percent in Fig. 9 (defined in s/h in percent in Fig. 2).

As the validation of the proposed FEM, the number of small elements increases in Fig. 10. The FEM uses the

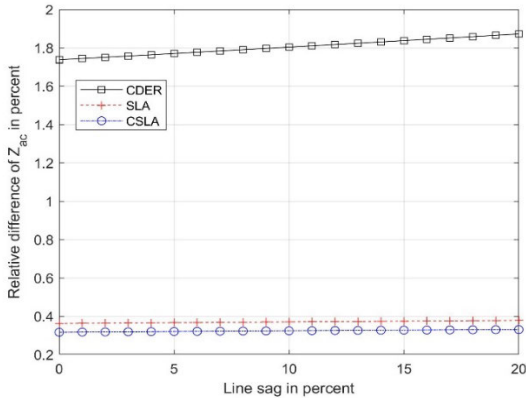


FIGURE 12. Relative difference of Z_{ac} to the reference when the sag ratio increases.

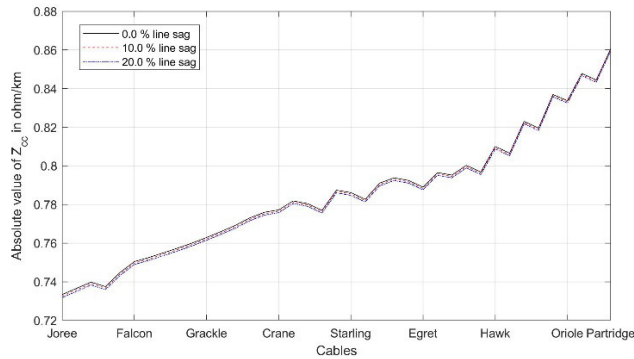


FIGURE 13. Absolute value of the self-impedance (Z_{cc}) when the cable changes.

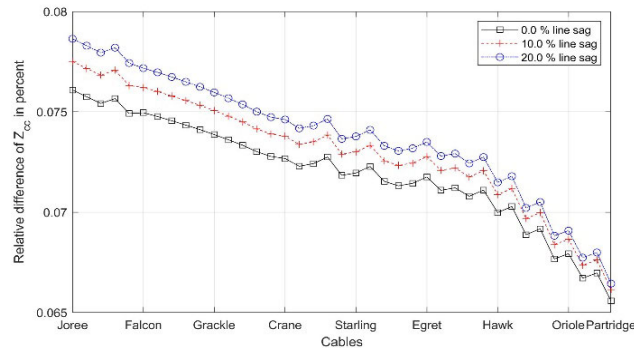


FIGURE 14. Relative difference of the self-impedance (Z_{cc}) to the reference when the cable changes.

compensated SLA method, or equations from (8) to (11). For the sag ratio of 20 percent, as the number of small elements increases, self-impedances (Z_{aa} , Z_{bb} , and Z_{cc}) converges to $0.2887 + 0.8094i$, $0.1069 + 0.7570i$, and $0.1452 + 0.7762i$ in Ω/km . Mutual impedances (Z_{ab} , Z_{ac} , and Z_{bc}) converge to $0.0494 + 0.2347i$, $0.0491 + 0.1825i$, and $0.0494 + 0.2347i \Omega/\text{km}$. As the sag ratio increases, the self- and mutual impedances decrease. It is because the more severely sagged, the closer conductors approach the ground. In other words, the GMD of the overhead line to its image conductor (e.g., D_{ij}

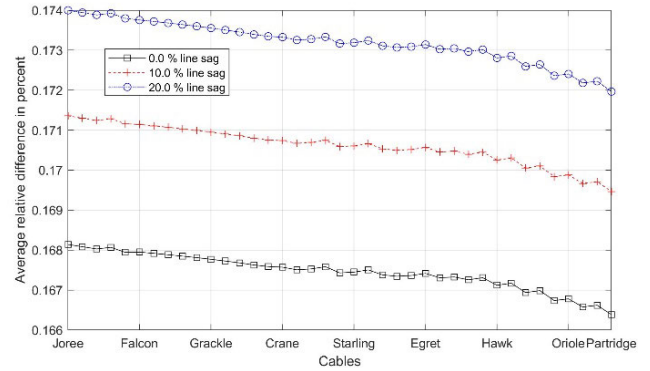


FIGURE 15. Average relative difference when the cable changes.

term in (3)) decreases, so the self- and mutual impedances decrease.

To analyze the effect of the line sag on the self- and mutual impedances of the OL, the sag ratio linearly increases from 0 to 20 percent. Fig. 11 and Fig. 12 indicate the absolute value and relative difference of the mutual impedance (e.g., Z_{ac}) when the line sag increases. In Fig. 11, as the sag increases, the absolute value of the mutual impedance decreases. If the overhead line is sagged, the GMD decreases, so the mutual impedance decreases. For the weakly sagged OL with a sag ratio of 20 percent, the mutual impedance calculated by the compensated SLA (denoted as CSLA with the diamond) is close to the reference impedance, denoted as the reference with the square, compared to the CDER and SLA methods, which is comparable to [8]. In Fig. 12, as the sag increases, the relative difference of the mutual impedance calculated by the compensated SLA slightly increases because the mutual impedance also decreases according to the sag. The self-impedance shows the same pattern as Fig. 11 and Fig. 12.

To analyze the effect of an imbalance in the phase conductors of the sagged OL on the self- and mutual impedances, the conductor of phase c changes from the first to the last ACSR cable in TABLE 1. The FEM also uses the compensated SLA method. In Fig. 13, as the cable changes from Joree to Partridge, the absolute value of the self-impedance of phase c (e.g., Z_{cc} in Ω/km) increases because the GMR of the conductor decreases and the dc resistance increases. For all the cables, a sag ratio of 20 percent decreases the absolute value of Z_{cc} . Fig. 14 presents the relative difference of self-impedance (Z_{cc}) to the reference, which decreases when the GMR of the conductor decreases and the dc resistance increases. The 20 percent sag also increases the relative difference of self-impedance (Z_{cc}). Fig. 15 indicate the average of the relative difference of self- and mutual impedances, which shows the same decreasing pattern as Fig. 14.

VII. CONCLUSION

The objective of this study is not only to find EVs of self- and mutual impedances of OLs with polyhedral uncertainties (e.g., the ground resistivity, overhead line structure, and cable) but also to examine the effects of an increase

in line sags (e.g., the sag ratio from 0 to 20 percent) and an imbalance in phase conductors on the self- and mutual impedances. For this purpose, this study designed a stochastic Monte Carlo simulation model and presented the two-step variable-sized FEM. As a result of the case studies, the EVs of the self- and mutual impedances of the ACSR OLs with various uncertainties are successfully evaluated. It was also shown that as the sag ratio increases, the self- and mutual impedances decrease. However, this study ignored not only other cable specifications (e.g., copper) in the Monte Carlo simulations but also heavily sagged overhead lines, which is the future work of this paper.

REFERENCES

- [1] J. R. Carson, "Wave propagation in overhead wires with ground return," *Bell Syst Tech. J.*, vol. 5, no. 4, pp. 539–554, 1926.
- [2] A. Weisshaar, P. C. Magnusson, V. K. Tripathi, and G. C. Alexander, *Transmission Lines and Wave Propagation*. Boca Raton, FL, USA: CRC Press, 2000.
- [3] Á. Déri and G. Tevan, "Mathematical verification of Dubanton's simplified calculation of overhead transmission line parameters and its physical interpretation," *Archiv für Elektrotechnik*, vol. 63, nos. 4–5, pp. 191–198, Jul. 1981.
- [4] C. Dubanton, "Calcul approché des paramètres primaires et secondaires d'une ligne de transport, valeurs homopolaires (approximate calculation of primary and secondary transmission line parameters, zero sequence values)," *EDF Bull. de la Direction des Études et Res.*, vol. 1, pp. 53–62, 1969.
- [5] A. Deri, G. Tevan, A. Semlyen, and A. Castanheira, "The complex ground return plane a simplified model for homogeneous and multi-layer earth return," *IEEE Trans. Power App. Syst.*, vol. PAS-100, no. 8, pp. 3686–3693, Aug. 1981.
- [6] C. Gary, "Approche complète de la propagation multifilaire en haute fréquence par utilisation des matrices complexes," *EDF Bull. de la Direction des Études et Recherches B, Réseaux Électr. Mater. Électr.*, vols. 3–4, p. 5, 1976.
- [7] F. L. Alvarado and R. Betancourt, "An accurate closed-form approximation for ground return impedance calculations," *Proc. IEEE*, vol. 71, no. 2, pp. 279–280, Feb. 1983.
- [8] I. Kim, "A new single-logarithmic approximation of Carson's ground-return impedances—Part 1," *IEEE Access*, vol. 9, pp. 103850–103861, 2021.
- [9] M. Pizarro and R. Eriksson, "Modeling of the ground mode of transmission lines in time domain simulations," in *Proc. 7th Int. Symp. High Voltage Eng.*, Dresden, Germany, 1991, pp. 179–182.
- [10] T. Noda, "A double logarithmic approximation of Carson's ground-return impedance," *IEEE Trans. Power Del.*, vol. 21, no. 1, pp. 472–479, Jan. 2006.
- [11] T. A. Papadopoulos, A. I. Chrysochos, C. K. Traianos, and G. Papagiannis, "Closed-form expressions for the analysis of wave propagation in overhead distribution lines," *Energies*, vol. 13, no. 17, p. 4519, Sep. 2020.
- [12] G. K. Papagiannis, D. A. Tsiमितros, D. P. Labridis, and P. S. Dokopoulos, "A systematic approach to the evaluation of the influence of multilayered earth on overhead power transmission lines," *IEEE Trans. Power Del.*, vol. 20, no. 4, pp. 2594–2601, Oct. 2005.
- [13] D. G. Triantafyllidis, G. K. Papagiannis, and D. P. Labridis, "Calculation of overhead transmission line impedances a finite element approach," *IEEE Trans. Power Del.*, vol. 14, no. 1, pp. 287–293, Jan. 1999.
- [14] G. K. Papagiannis, D. G. Triantafyllidis, and D. P. Labridis, "A one-step finite element formulation for the modeling of single and double-circuit transmission lines," *IEEE Trans. Power Syst.*, vol. 15, no. 1, pp. 33–38, Feb. 2000.
- [15] X. Dong, "Analytic method to calculate and characterize the sag and tension of overhead lines," *IEEE Trans. Power Del.*, vol. 31, no. 5, pp. 2064–2071, Oct. 2016.
- [16] Y. Yang, J. Lu, and Y. Lei, "A calculation method for the electric field under double-circuit HVDC transmission lines," *IEEE Trans. Power Del.*, vol. 23, no. 4, pp. 1736–1742, Oct. 2008.
- [17] A. V. Mamishev, R. D. Nevels, and B. D. Russell, "Effects of conductor sag on spatial distribution of power line magnetic field," *IEEE Trans. Power Del.*, vol. 11, no. 3, pp. 1571–1576, Jul. 1996.
- [18] A. Z. E. Dein, "Magnetic-field calculation under EHV transmission lines for more realistic cases," *IEEE Trans. Power Del.*, vol. 24, no. 4, pp. 2214–2222, Oct. 2009.
- [19] F. Moro and R. Turri, "Fast analytical computation of power-line magnetic fields by complex vector method," *IEEE Trans. Power Del.*, vol. 23, no. 2, pp. 1042–1048, Apr. 2008.
- [20] L. Hofmann, "Series expansions for line series impedances considering different specific resistances, magnetic permeabilities, and dielectric permittivities of conductors, air, and ground," *IEEE Trans. Power Del.*, vol. 18, no. 2, pp. 564–570, Apr. 2003.
- [21] A. Polevoy, "Impact of data errors on sag calculation accuracy for overhead transmission line," *IEEE Trans. Power Del.*, vol. 29, no. 5, pp. 2040–2045, Oct. 2014.
- [22] D. Fang, M. Zou, G. Coletta, A. Vaccaro, and S. Z. Djokic, "Handling uncertainties with affine arithmetic and probabilistic OPF for increased utilisation of overhead transmission lines," *Electr. Power Syst. Res.*, vol. 170, pp. 364–377, May 2019.
- [23] M. Grbić, J. Mikulović, and D. Salamon, "Influence of measurement uncertainty of overhead power line conductor heights on electric and magnetic field calculation results," *Int. J. Electr. Power Energy Syst.*, vol. 98, pp. 167–175, Jun. 2018.
- [24] T. Theodoulidis, "On the closed-form expression of Carson's integral," *Periodica Polytech. Electr. Eng. Comput. Sci.*, vol. 59, pp. 26–29, Apr. 2015.
- [25] E. L. Wachspress, *A Rational Finite Element Basis*. Amsterdam, The Netherlands: Elsevier, 1975.
- [26] D. Braess, *Finite Elements: Theory, Fast Solvers, and Applications in Elasticity Theory*. Cambridge, U.K.: Cambridge Univ. Press, 2007.
- [27] H. W. Dommel, *Electromagnetic Transients Program (EMTP) Theory Book*. Vancouver, BC, Canada: Microtran Power System Analysis Corporation, 1996.
- [28] I. Kim, "An approximate model for calculating three-phase line series impedance using the knee point selection method," *Int. Trans. Electr. Energy Syst.*, vol. 31, no. 4, 2021, Art. no. e12808.
- [29] J. Duchi, "Optimization with uncertain data," Dept. Elect. Eng., Stanford Univ., Stanford, CA, USA, Notes EE364b, 2018.
- [30] J. D. Glover, M. Sarma, and T. Overbye, *Power System Analysis and Design*. Boston, MA, USA: Cengage Learning, 2011.
- [31] A. R. Bergen and V. Vittal, *Power Systems Analysis*, 2nd ed. Upper Saddle River, NJ, USA: Prentice-Hall, 2000.
- [32] California Public Utilities Commission. (Jan. 3, 2013). *Transmission Structures*. [Online]. Available: <https://www.cpuc.ca.gov/Environment/info/aspenc/ctlp/additional.htm>



INSU KIM (Member, IEEE) received the Ph.D. degree from Georgia Institute of Technology, Atlanta, GA, USA, in 2014. He is currently an Associate Professor of electrical engineering with Inha University, South Korea. His major research interests include 1) analyzing the impact of stochastically distributed renewable energy resources, such as photovoltaic systems, wind farms, and microturbines on distribution networks; 2) examining the steady-state and transient behavior of distribution networks under active and reactive power injection by distributed generation systems; and 3) improving power-flow, short-circuit, and harmonic analysis algorithms.

...